Conf-870610--5

A SIMPLE CANTILEVERED MIRROR FOR FOCUSING SYNCHROTRON RADIATION*

Gene E. Ice and Cullie J. Sparks†

Metals and Ceramics Division
Oak Ridge National Laboratory
Oak Ridge, Tennessee 37831

CONF-870610--5

DE87 011679

Synchrotron Radiation Instrumentation

5th National Conference

University of Wisconsin-Madison

Madison, Wisconsin

June 21–25, 1987

*Research sponsored by the Division of Materials Sciences, U.S. Department of Energy, under contract DE-AC05-84OR21400 with the Martin Marietta Energy Systems, Inc.

†4500S, P. O. Box X, Oak Ridge, Tennessee 37831-6117, (615) 624-6996.

A SIMPLE CANTILEVERED MIRROR FOR FOCUSING SYNCHROTRON RADIATION*

Gene E. Ice and Cullie J. Sparks†

Metals and Ceramics Division
Oak Ridge National Laboratory
Oak Ridge, Tennessee 37831

A large cantilevered mirror was constructed to focus the vertical divergence from a synchrotron radiation source. The advantages of this mirror are its compactness, simple bending device, simplicity of construction, and good thermal contact to structures outside the vacuum. The central portion of the mirror is supported with variable loading springs to reduce gravitational sag. The figure and thermal stability of the mirror have proven to be excellent, though the focusing is limited by the roughness of the mirror-surface. This paper describes the design, construction, and performance of the mirror.

1. INTRODUCTION

Glancing angle mirrors have been widely used to focus X rays [1,2,3]. If a fixed critical angle can be assumed, then the required shape can be cut and polished into the surface of the mirror. The mirror then can be made extremely stiff to minimize deformation from gravitational sag and thermal or mechanical stress. However, if the critical angle is to be adjusted, then the radius of curvature R_m of the mirror also must be changed to achieve a good focus according to the following relationship:

---

*Research sponsored by the Division of Materials Sciences, U.S. Department of Energy, under contract DE-AC05-84OR21400 with the Martin Marietta Energy Systems, Inc.

$$R_m = \frac{2F_1F_2}{(F_1 + F_2)\sin\theta_c} \qquad (1)$$

where F_1 and F_2 are the object and image distances, and θ_c is the critical angle for specular reflection. A mirror with an adjustable radius, therefore, must be designed stiff enough to avoid unacceptable distortions, but flexible enough so that it can be bent within its elastic range.

For X-ray mirrors with surfaces coated with heavy metals, the critical angles for total external reflection are very small, on the order of θ_c = 0.1/E (keV). Here, E is the X-ray energy in keV. For such small critical angles, the meridioal radii are very large [Eq. (1)], hence the bending formula is well approximated by:

$$R = YI/M \qquad (2)$$

where Y is Young's modulus, M is the applied moment, and I is the second moment of the cross section of the mirror, equal to $\omega T^3/12$ for a rectangular cross section of width ω and thickness T.

In many cases, the ideal focusing shape is well approximated by a cylinder. Two bending schemes are routinely employed to achieve cylindrical curvatures on X-ray mirrors. These are four-point loading and cantilevered bending, Fig. 1(a) and 1(b). Four-point loading achieves a constant radius of curvature when a constant bending moment is generated between the central bending rods and when the mirror's cross section is constant along its length. An advantage of four-point loading is that it is ideal for bending long cylindrical mirrors to achieve a doubly-focusing toroid [4]. A disadvantage of four-point loading is the sensitivity of the curvature to small displacements between the loading points. Consequently, the curvature is sensitive to thermal variations which increases the complexity and cost of a four-point bending scheme.

In a cantilevered design, the applied moment M increases linearly with distance from the free end of the mirror, Fig. 1(b). Constant curvature is obtained by varying the cross section to compensate for the changing bending moment. Typically, the width ω is varied linearly (in the case of a triangular shaped mirror), but we have chosen the more compact design achieved by varying the thickness T. In general, a cantilevered design requires a smaller bending force and larger displacement of the bending mechanism to give a curvature similar to a four-point loaded design. Therefore, a cantilevered system is less sensitive to thermal variations and so simplifies the design of the bending mechanism.

2. DESIGN CRITERIA

Our mirror was designed to focus the vertical divergence emitted by the National Synchrotron Light Source (NSLS) X-ray ring [5]. The 4σ object size is approximately 1.0 mm horizontal by 0.4 mm vertical. The mirror is placed 7 m from the source and 11 m from the plane of the image. In addition to 0.4 mrad of vertical divergence, the mirror must intercept 15 mrad of horizontal divergence which is focused downstream by a sagittally focusing Si (111) crystal [6]. The thermal load on the mirror can be expected to reach 600 W. The critical energy for specular reflection from the mirror must be adjustable from 5 to 40 keV. With a platinum mirror surface, this required an adjustable critical angle within θ_c of 2 to 15 mrad and an adjustable radius of curvature of 4.3 to 0.57 km. For good X-ray reflectivity, a surface roughness of less than 10Å RMS is needed [7].

3. MIRROR DESIGN AND FABRICATION

The mirror blank was cut from a monolithic block of disk-grade 5086 aluminum. The reflecting surface of the mirror is rectangular, 12 cm x 68 cm, and the thickness of the mirror has a cube-root dependence, with distance from the free end varying from a maximum of 5 cm to a minimum of 2.5 cm (Fig. 2). The central 50 cm of the mirror has a thickness which increases as the cube root of the distance from the point of applied bending force. The mirror blank was bored for cooling channels. The calculated effect of cooling channels on the bending moment of the mirror is negligible. Similarly, the calculated distortions of the surface with two atmospheres pressure in the cooling channels is negligible. The blank was inspected, heat-treated, and machined to 0.025 mm tolerance. The mirror was given an optical polish and then coated with electroless nickel. Following a final heat treatment, the nickel was super-polished. Finally, a platinum reflecting layer was applied using a proprietary process developed by Applied Optics. Earlier tests showed no difference between the surface roughness of super-polished nickel blanks before and after being platinum-coated by vapor deposition or by the Applied Optics proprietary method [8].

The mirror was bolted to a 10 in. stainless steel flange and the mirror's cooling paths were connected to the mounting flange, (Fig. 2). Thermocouples were attached to the mirror to measure temperature changes and the entire assembly was bolted onto a UHV tank. The springs then were adjusted to support the mirror and reduce gravitational sag [9]. A UHV translator under the free end of the mirror provides the bending moment through a roller bearing (Fig. 3). All alignments and displacements of the mirror are accomplished by moving the tank to which the mirror is rigidly attached (Fig. 3).

4. GRAVITATIONAL SAG CORRECTION

The thickness of the mirror blank was limited to keep the bending stress below that for plastic deformation and to reduce the bending forces to achieve the minimum radius of approximately 500 m. This thickness would permit gravitational sag to be significant. To compensate for the gravitational sag, we supported the mirror by suitably placed springs with variable loading. Since the displacement of the mirror during bending is small, changes in the spring tension are slight. Thus, gravitational sag, once removed at a single critical angle, is removed under all operating conditions.

5. MEASUREMENT OF SURFACE FIGURE

The flatness of the unbent mirror blank was measured by the vendor with a Twymann-Green unequal path interferometer having a 24 in. collimator. Because of the size of the mirror, two overlapping interferograms were required. The deviation of the overall surface from a flat was less than 2.5 arcseconds. RMS slope errors of less than 2 arcseconds are needed to image the NSLS source with negligible blurring for the focal distances of below 10 m.

The figure error of the bent mirror, corrected for gravitational sag, was measured by Takacs [9]. The deviations from a cylindrical curvature were less than 2.5 arcseconds, agreeing with the results reported by the vendors. These errors were slightly reduced by applying sag correctors (Fig. 4).

After exposure to the white radiation of the NSLS X-ray ring for approximately 6000 exposure hours, the mirror surface was measured and inspected again for overall flatness by Continental Optics, on an 18 in. unequal path interferometer. The mirror blank was measured bolted onto its mounting flange. There was no distortion of the surface of the mirror near the mounting flange, but the overall figure showed a mean radius of ≈10 km. This represented a substantial change from the original figure. Fortunately, the curvature was opposite in sign from that required for focusing and could, therefore, be removed by applying a slightly greater bending force. This change in figure is inexplicable since any plastic deformation of the mirror from bending should be opposite in sign from the observed curvature. No degradation of the surface finish nor deposit was observed.

6. SURFACE FINISH AND X-RAY PERFORMANCE

The reflectivity of the mirror under various operating conditions was determined by monitoring the integrated flux through a 2.5 cm aperture sited 7 m from the mirror. The reflectivity at 8.333 keV and 6 mrad glancing angle was only 35%. For an ultra-smooth mirror with negligible scattering due to surface roughness, the integrated reflectivity of a platinum surface should exceed 90%. The 8.333 keV reflectivity was improved to 67% by going to a glancing angle of 3 mrad. This result is what would be expected if surface roughness is responsible for poor reflectivity. An estimate of the dependence of focused reflectivity on glancing angle and surface roughness is given by:

$$R = e^{-(4\pi\sigma\frac{\theta}{\lambda})^2} \tag{3}$$

where λ is the X-ray wavelength, σ is the RMS surface roughness, θ is the glancing angle in radians and R is the reflectivity into the focus. From this formula, we calculate an RMS roughness between 21–26Å.

Despite this poor reflectivity, a focal spot only about 50% larger than that for ideal imaging was achieved. The best measured vertical spot size was found to be 0.96 mm 4σ, compared to an ideal size of 0.61 mm based on pinhole imaging of the electon beam [10]. In the collimating mode, a beam with a full-width half-maximum divergence of 1.8×10^{-4} was obtained. By comparison, the opening angle of the source is about 4×10^{-4}, and the source size-limited divergence for a perfect collimating mirror located 7 m from the source is 6×10^{-5}. Figure 5(a) shows the best vertical beam focus. Figure 5(b) shows the best beam collimation when the entire vertical divergent is accepted.

The disappointing reflectivity and imaging of the mirror are attributed primarily to a faceted surface. Scans of the focus with a 0.5 mm slit that samples various regions of the mirror's surface show small angle scattering (Fig. 6).

The RMS surface roughness was measured by Takacs using a WYKO NCP 1000 5 mm profilometer [9]. The surface roughness for spatial frequencies below 5 mm was found to range between 21 and 28Å with most regions having about 24Å RMS roughness. Especially distinctive were diamond shaped facets visible on the mirror surface which may be a print through the nickel coating of the original aluminum surface fly cutting. More recent results on other polished nickel coated mirrors show that smoother surfaces are now possible.

7. THERMAL STABILITY

The thermal stability of the mirror was followed over two years of operations by monitoring energy shifts caused by changes in the x-ray angles incident on a two-crystal monochromator, and by observing shifts in the position of the image. These measurements cannot be uncoupled from changes in the orbit of the electron beam nor from the instabilities of the monochromator. Nevertheless, periods of extreme stability were observed which were attributed to stability of the electron beam, the mirror, and the monochromator. For example, the three-day run illustrated in Fig. 7 shows less than 15 μrad angular shifts during and between fills. This performance was recorded with beam currents cycling between 50 and 200 mA and indicates good thermal stability for the mirror.

8. CONCLUSION

The cantilevered mirror constructed for the ORNL X-ray beamline makes the mirror system inexpensive to construct and gives it good stability and adjustability.

REFERENCES

1. P. Kirkpatrick and A. V. Baez, J. Opt. Soc. of Am. 38, (1948) 766.
2. J. Hendrix, M.H.J. Koch, and J. Bordas, J. Appl. Cryst. 12, (1979) 467.
3. S. M. Heald and J. B. Hastings, Nucl. Inst. and Methods 195, (1982) 59.
4. J. A. Howell and P. Horowitz, Nucl. Inst. and Methods 125, (1975) 225.
5. A. Van Steenbergen and NSLS Staff, Nucl. Inst. and Methods 172, (1980) 25.
6. A. Habenschuss, G. E. Ice and C. J. Sparks, X-ray Optics and Performance of a 3-40 keV X-ray Scattering Beamline at the National Synchrotron Light Source, (1987), to be published in these proceedings.
7. E. L. Church and P. Z. Takacs, BNL Report No. 37880 (1985).
8. J. Isenberger and M. R. Howells, BNL Informal Report No. 33868 (1983).
9. P. Takacs and J. Colbert, Nucl. Inst. and Methods A246, (1986) 223.
10. NSLS 1985 Annual Report, BNL Report No. 51947, (1985) 167.

FIGURE CAPTIONS

FIGURE 1. Illustration of two techniques to generate a cylinder. In the case of four point loading, the figure developed is a cylinder when the opposing moments are equal and the beam cross section is uniform. For the cantilevered case, the thickness of the bent beam must vary like $\ell^{1/3}$ to develop a cylindrical curvature.

FIGURE 2. ORNL cantilevered mirror with mounting flange. Cooling paths are seen connected to the flange. These paths were never used because of NSLS vacuum rules. Water cooling of the flange was used during operations.

FIGURE 3. Schematic of the ORNL mirror and mirror tank. The tilt of the mirror tank can be adjusted by a linear translator located at the point labeled A. This translator acts through a ball and slide arrangement at A causing the mirror tank to rotate around a flex pivot located at the point labeled B. To change the mirror tank height, the translators at A and B are driven together. Since the mirror is rigidly attached to the mirror tank, these mirror tank adjustments are used to adjust the critical angle of the mirror, and to center the mirror in the X-ray beam. The curvature of the mirror is adjusted by driving a UHV translator indicated at the point C. Also shown in the schematic are the support springs used to reduce gravitational sag of the mirror.

FIGURE 4. Interference patterns with and without gravitational sag correction. As seen in the patterns, the addition of gravitational sag correction improves the symmetry of the pattern indicating the improvement of the mirror's overall figure.

FIGURE 5A. Vertical focus of the X14A X-ray beam at magnification of 1.6. The background under the peak is attributed to small angle scattering.

FIGURE 5B. Vertical collimation of the X14A X-ray beam as measured by a antiparallel Si (111) crystal at the target position.

FIGURE 6. Vertical intensity distribution of radiation reflected from selected regions of the ORNL cantilevered mirror. These measurements were made by scanning a 0.1 mm slit vertically in front of a wide open detector at the image point. To study the scatter from different parts of the mirror surface, a pre-mirror slit with a 0.5 mm opening was scanned vertically in 0.25 mm steps. This figure shows the scattered intensity from three representative regions of the mirror surface. The 0.25 mm slit is shown in step 2 of the 6 steps.

FIGURE 7. Repeated scans of the iron edge taken over 36 hours show very small shifts, indicating stable mirror performance. During this period, the electron current cycled from 200 to 50 ma.

FOUR POINT LOADING

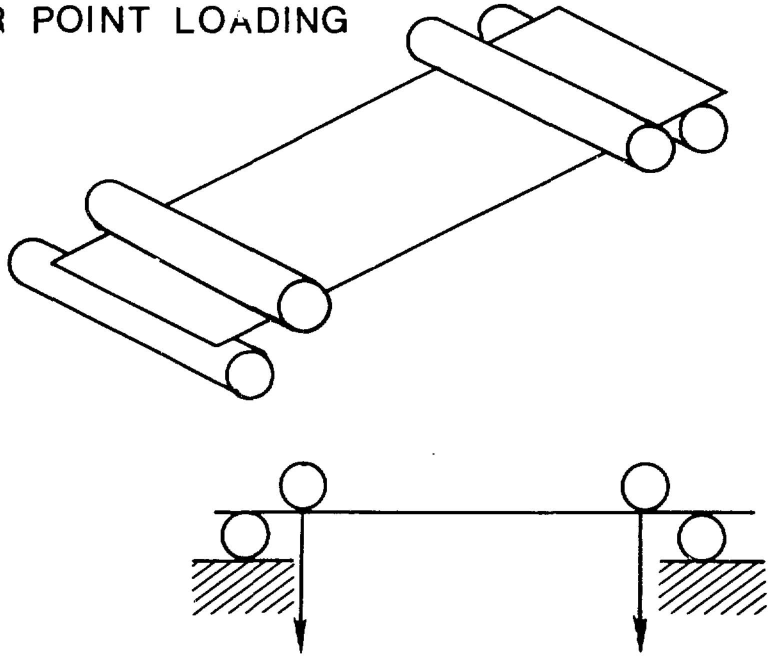

CANTILEVERED

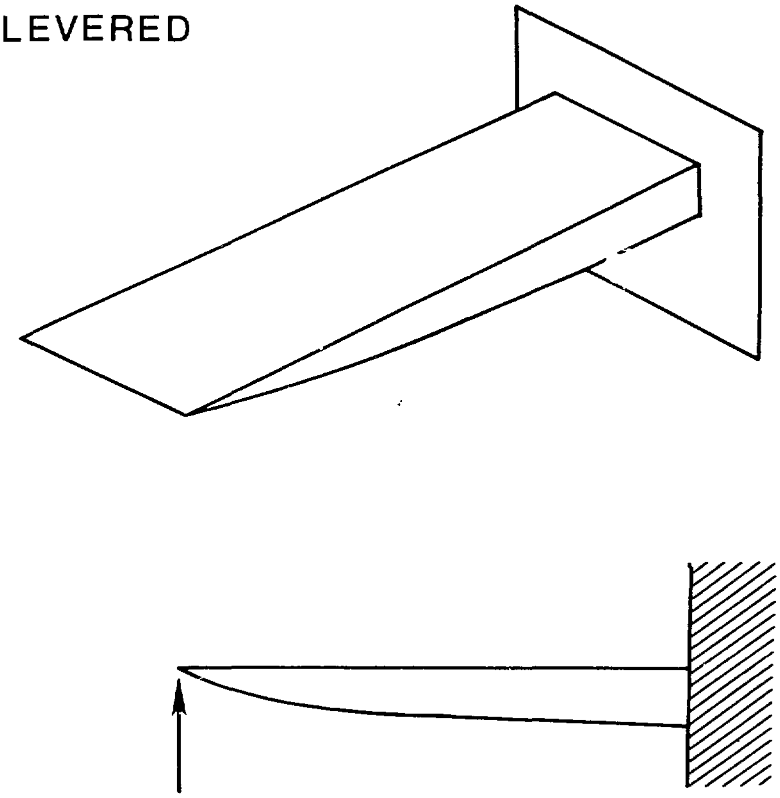

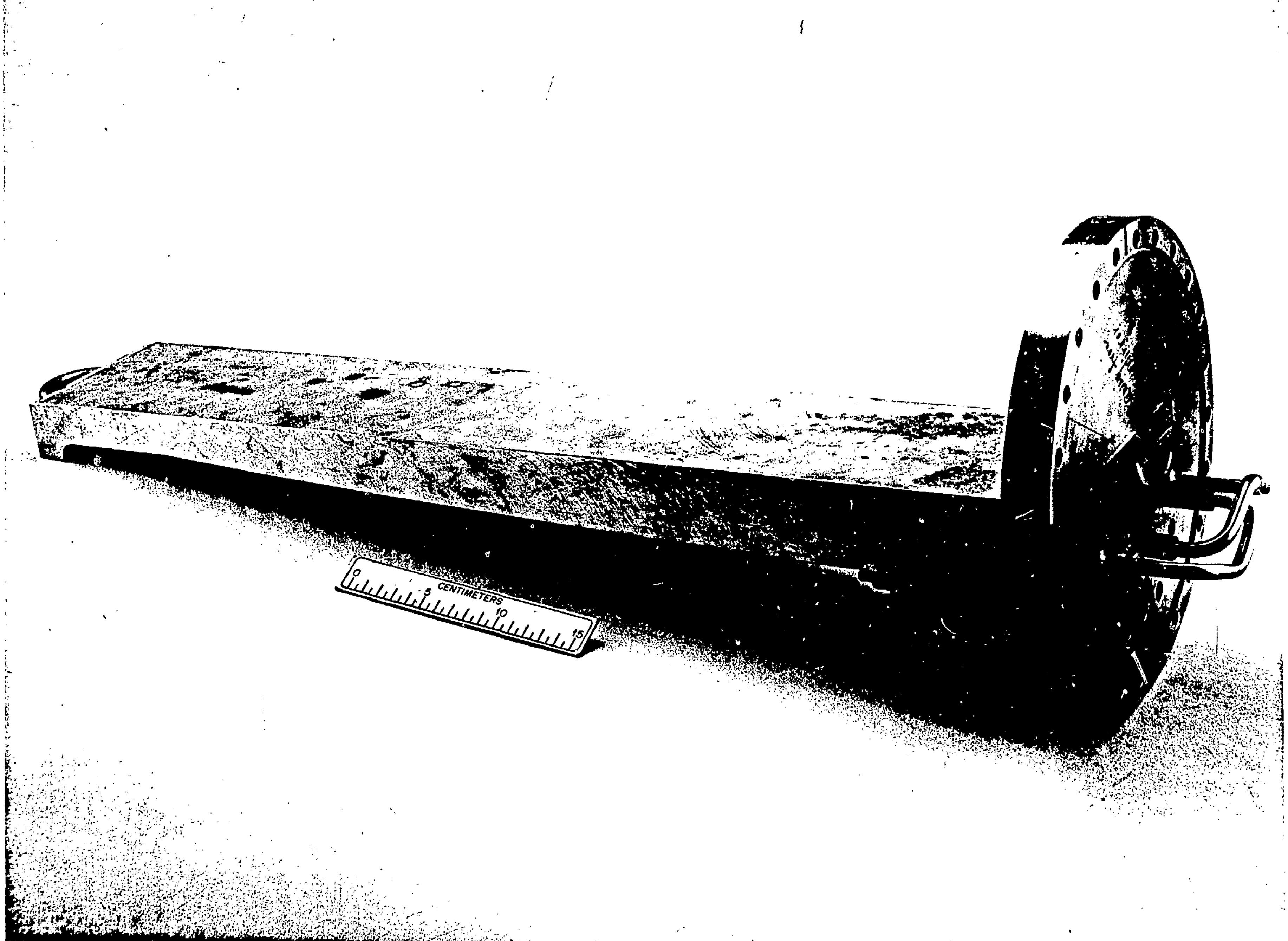
CENTIMETERS
0
5
10
15

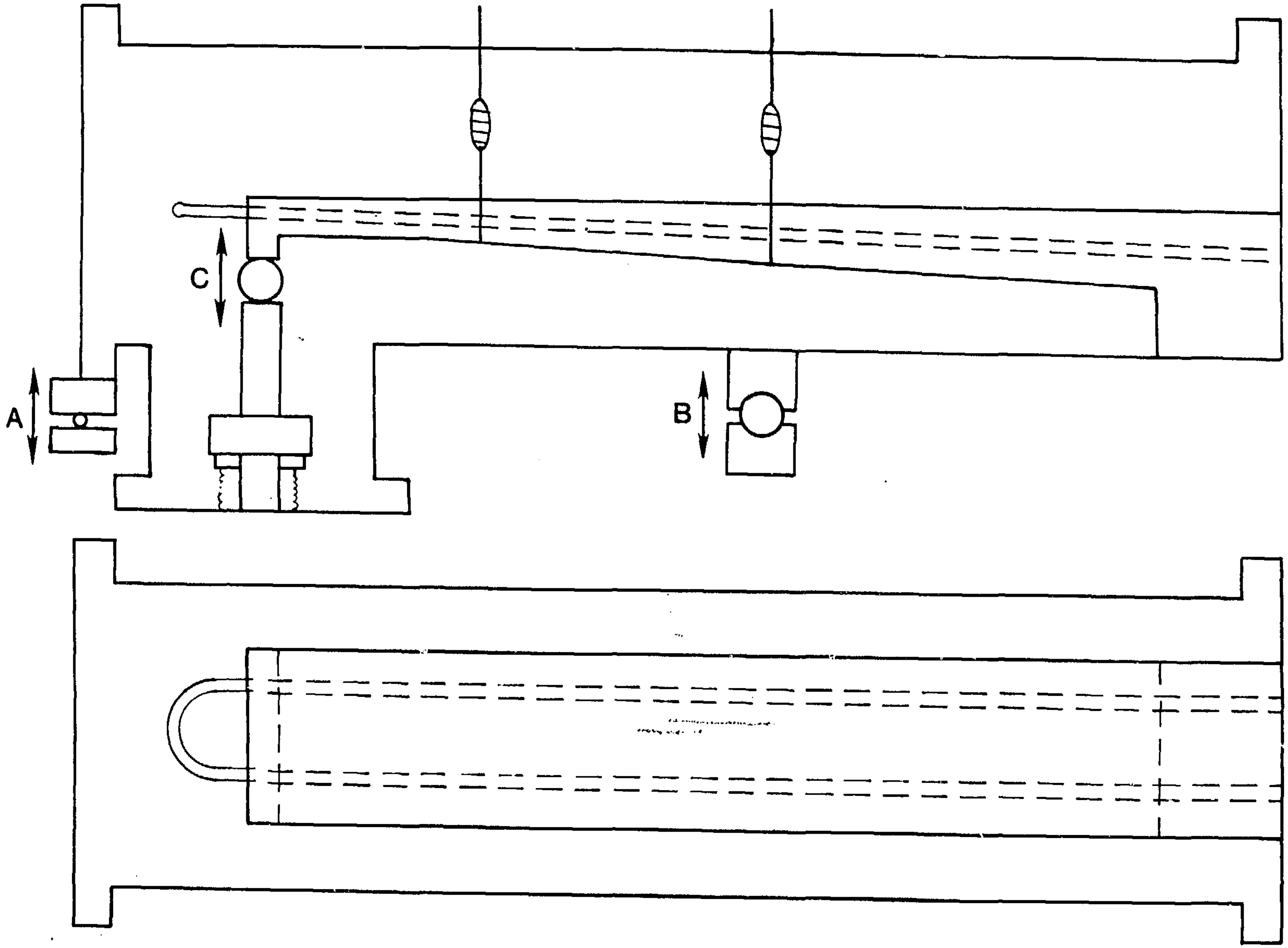
C
A
B

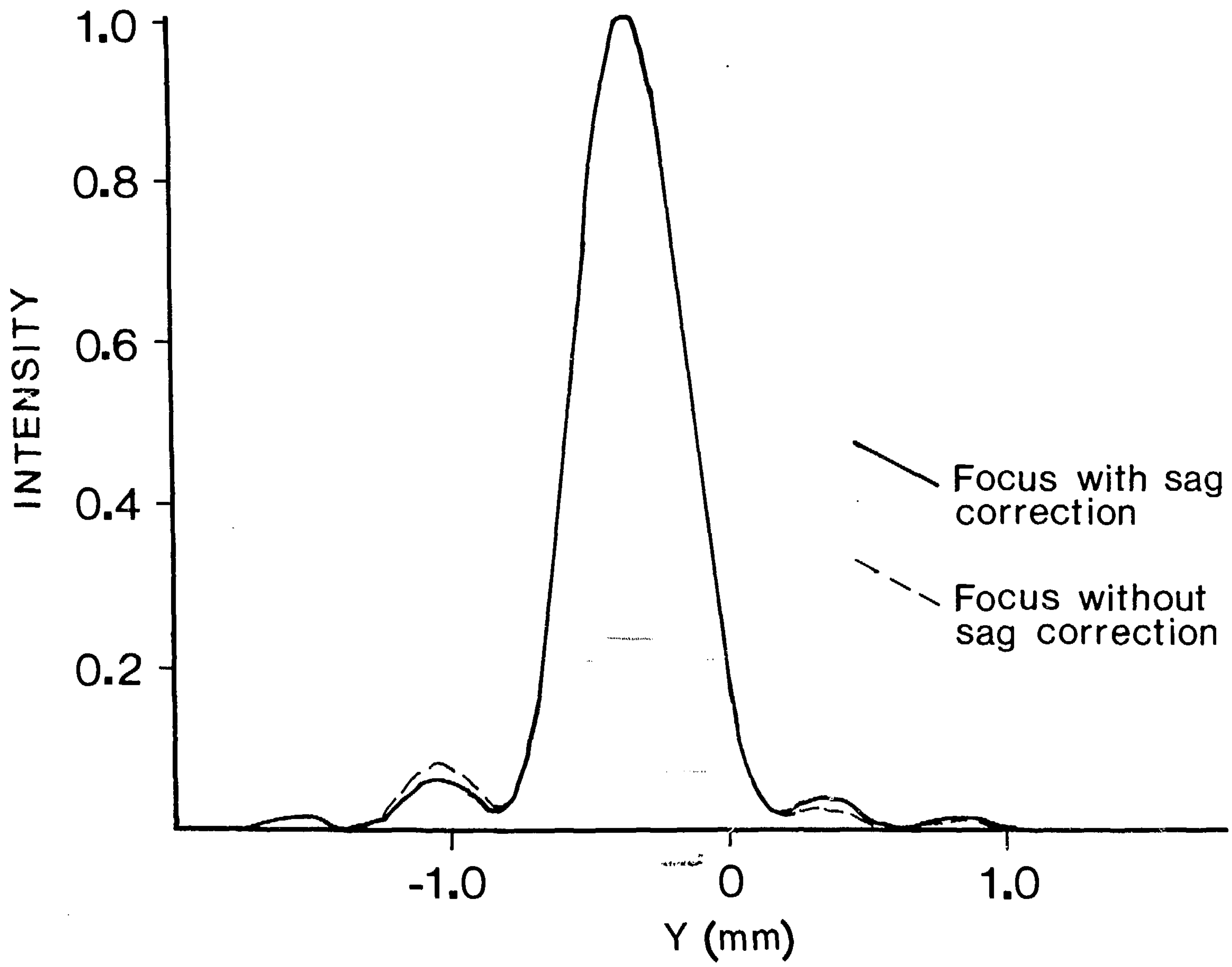

1.0
0.8
0.6
0.4
0.2
INTENSITY
-1.0
0
1.0
Y (mm)
Focus with sag correction
Focus without sag correction

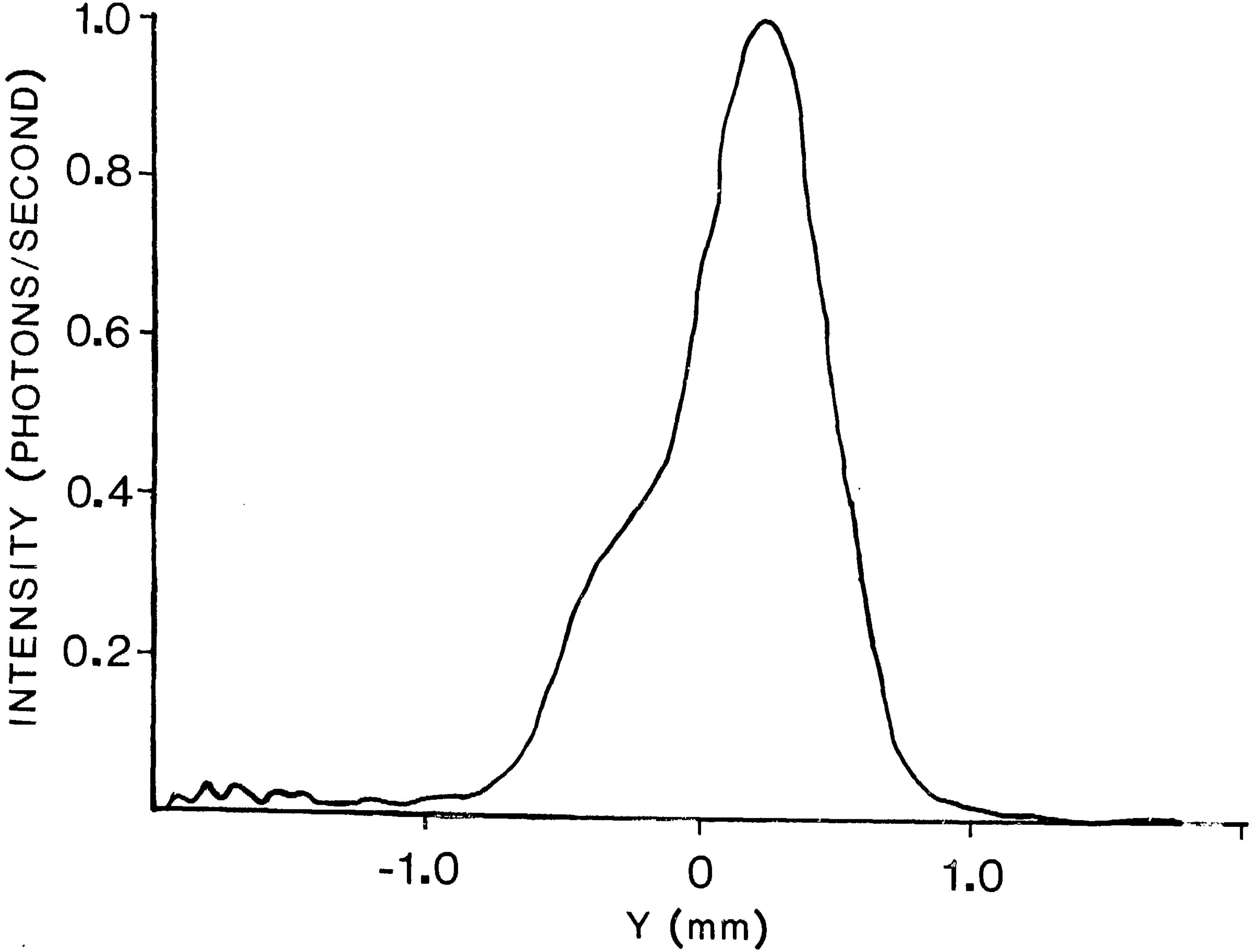
INTENSITY (PHOTONS/SECOND)
1.0
0.8
0.6
0.4
0.2
-1.0
0
1.0
Y (mm)

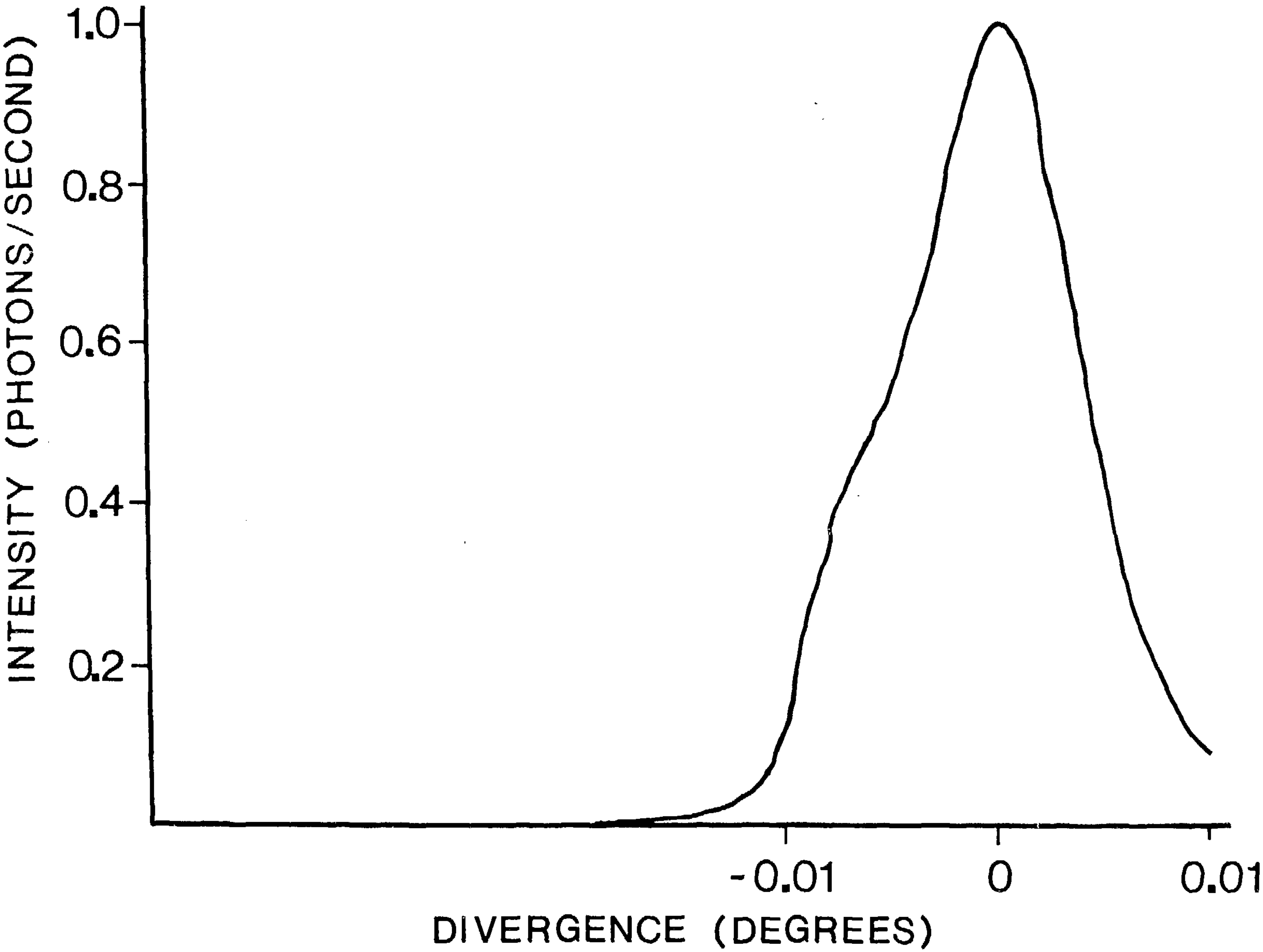
1.0
0.8
0.6
0.4
0.2
INTENSITY (PHOTONS/SECOND)
-0.01
0
0.01
DIVERGENCE (DEGREES)

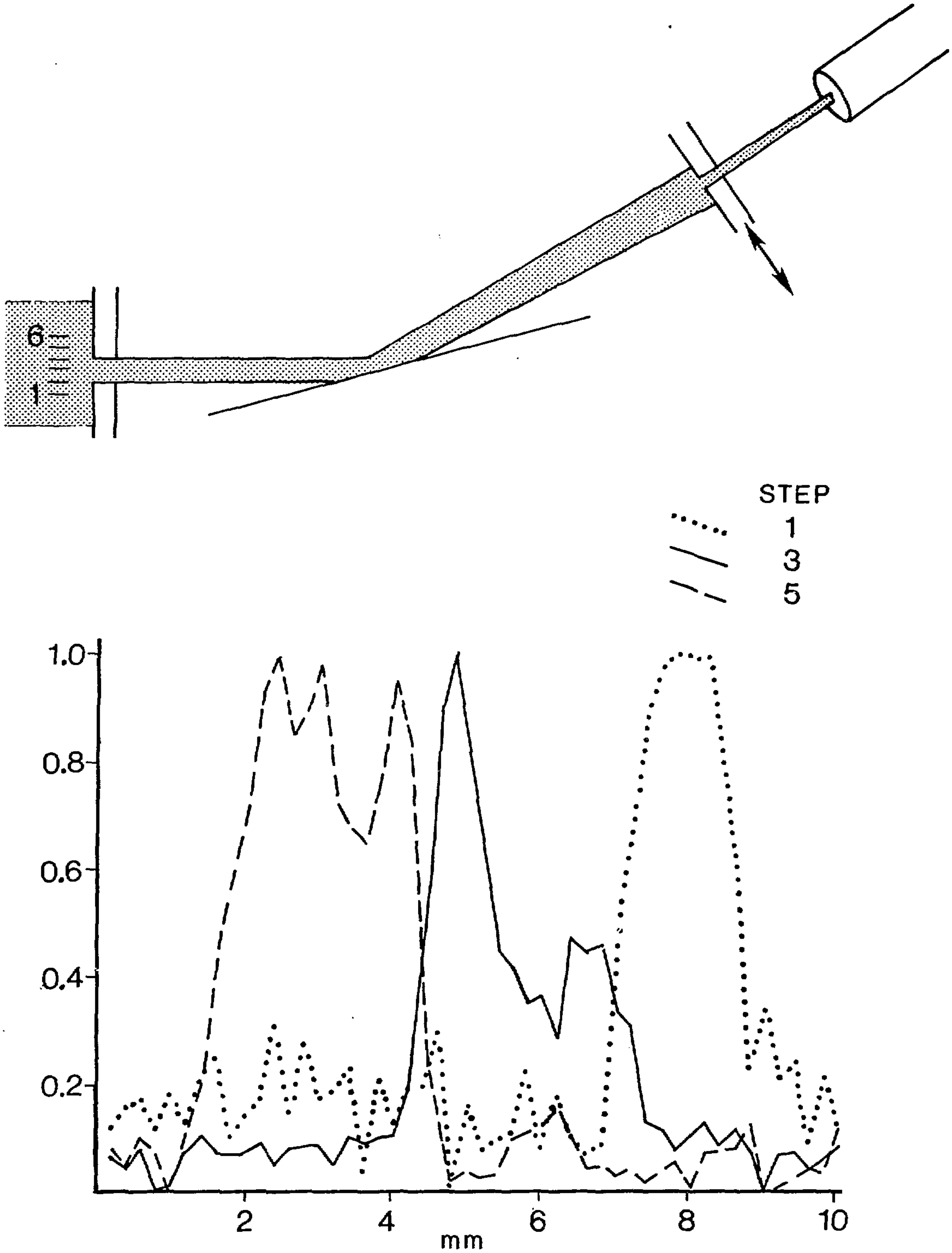
6
1
STEP
1
3
5
1.0
0.8
0.6
0.4
0.2
2
4
6
8
10
mm

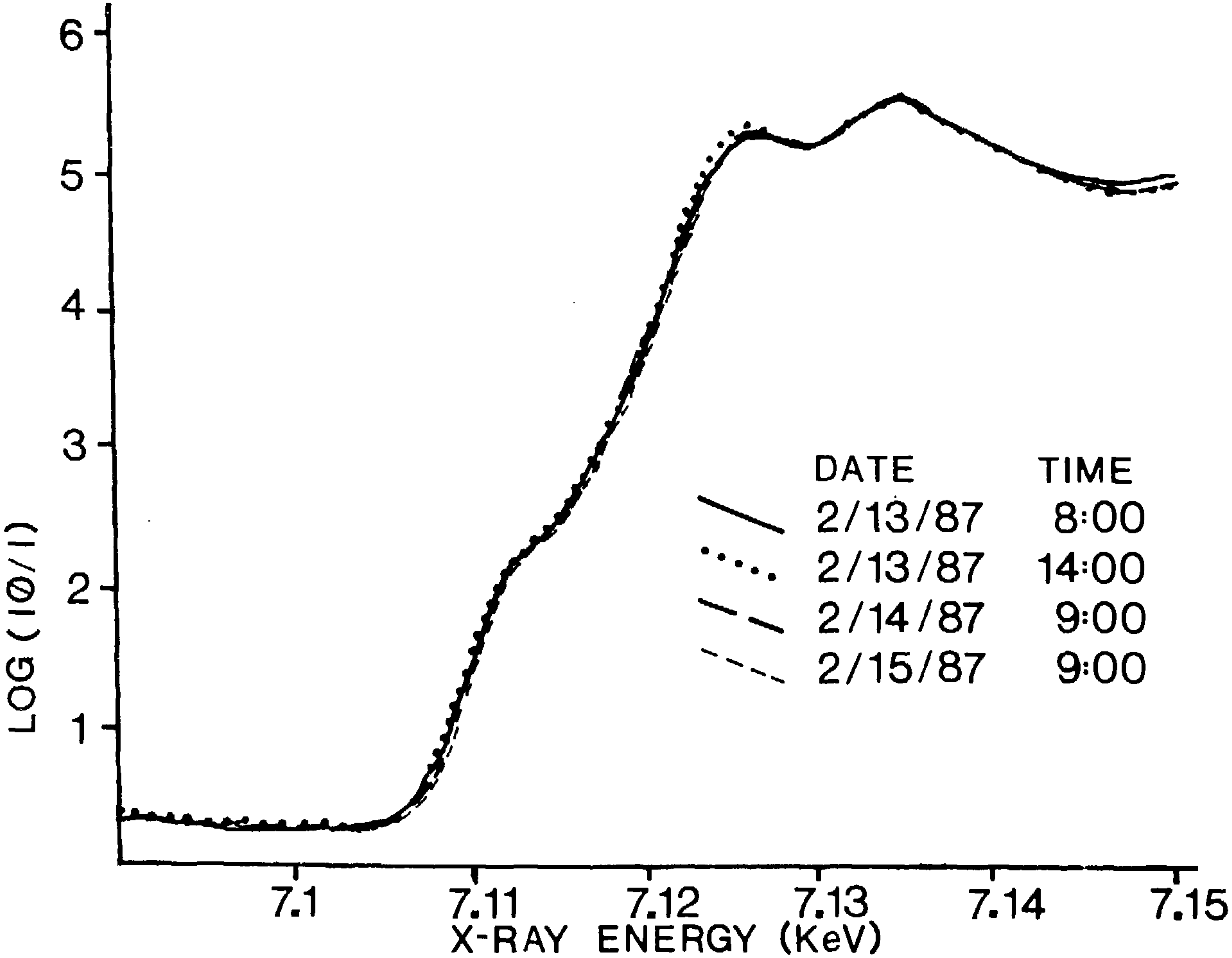

LOG (IØ/I)
6
5
4
3
2
1
7.1
7.11
7.12
7.13
7.14
7.15
X-RAY ENERGY (KeV)
DATE TIME
2/13/87 8:00
2/13/87 14:00
2/14/87 9:00
2/15/87 9:00